

A Diode Laser Study of the NCO + NO₂ Reaction

Joonbum Park and John F. Hershberger*

Department of Chemistry, North Dakota State University, Fargo, North Dakota 58105

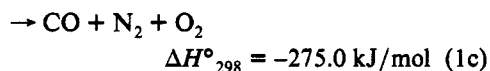
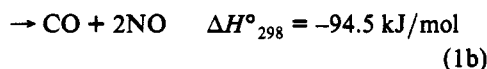
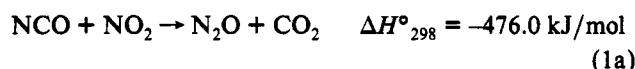
Received: July 29, 1993; In Final Form: October 1, 1993*

Infrared diode laser absorption spectroscopy was used to investigate the kinetics and product channels of the NCO + NO₂ reaction. The total rate constant was fit to the form $k = 10^{-11.38 \pm 0.06} \exp[(441 \pm 53)/T]$ over the temperature range 298–500 K. The major product channel was CO₂ + N₂O, accounting for $91.7 \pm 4.0\%$ of the total observed products; CO + 2NO accounted for the remaining $8.3 \pm 4.0\%$. The energy disposal into the ν_3 mode of the CO₂ product was also measured. A value of $\langle f_{\nu_3} \rangle = 5.9 \pm 2.0\%$ was determined. The results are consistent with formation of a long-lived O₂NNCO collision complex with a roughly statistical distribution of internal energy. Concerted dissociation via a four-center transition state leads to the primary products.

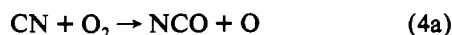
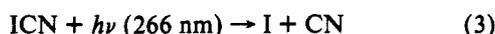
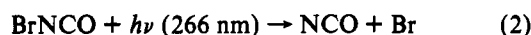
Introduction

Reactions of the NCO radical have received substantial interest due to the role this species plays in the combustion chemistry of nitrogen, especially the RAPRENO_x and other NO_x control strategies.^{1–4} The kinetics of NCO reactions with several species, including NO, O, O₂, H₂, and C₂H₄, have been previously measured.^{5–11}

In this paper, we report measurements of the kinetics and product channel dynamics of the NCO + NO₂ reaction. Several product channels are possible:



The thermodynamic data have been calculated using $\Delta H_f^\circ(\text{NCO}) = 131.4 \text{ kJ/mol}$ ¹² and standard values of ΔH_f° for the other species.¹³ NCO radicals are produced in our experiment by direct laser photolysis of a halogen isocyanate (BrNCO) or indirectly by photolysis of ICN followed by reaction of CN with O₂ or NO₂:



Reactions 4 and 5 are quite fast. Several workers^{14–16} have measured k_4 to be $(1.8\text{--}3.0) \times 10^{-11} \text{ cm}^3 \text{ molecule}^{-1} \text{ s}^{-1}$. In a previous paper,¹⁷ k_5 was measured to be $9.3 \times 10^{-11} \text{ cm}^3 \text{ molecule}^{-1}$

s^{-1} , with branching ratios of 86.8%, 7.6%, and 5.6% for channels 5a, 5b, and 5c, respectively, at room temperature.

Experimental Section

The experimental technique has been described in detail previously.^{17–19} Only a brief description will therefore be given here. The 266-nm fourth harmonic of a Lumonics JK750 Nd:YAG laser was used as the photolysis source. NCO radicals and CO, CO₂, NO, and N₂O product molecules were probed by time-resolved infrared absorption spectroscopy using a tunable diode laser spectrometer. The probe and photolysis beams were made collinear by a dichroic mirror and copropagated through the reaction cell. Iris diaphragms (6-mm diameter) were used at each end of the cell to ensure good beam overlap. The infrared radiation was then transmitted through a $1/4$ -m monochromator and detected by an InSb infrared detector (Cincinnati Electronics). Transient absorption signals were collected on a digital oscilloscope (Hitachi 6065) and stored in a personal computer for later analysis.

Room temperature experiments were performed using a 145-cm single-pass Pyrex absorption cell. A 67-cm resistively heated Pyrex cell was used for experiments at elevated temperatures. Cell temperature was measured using Type J thermocouples; accuracy and uniformity of $\pm 5 \text{ K}$ are estimated. Calibration of diode laser frequencies was performed using CO, CO₂, NO, and N₂O reference gases and tabulated line positions.^{20,21} A high-voltage dc discharge was used in order to locate excited-state spectral lines of CO, NO, and CO₂. NCO spectral lines in the ν_3 band near 1910 cm^{-1} were found with the aid of recent assignments.²² The reaction cell was evacuated and refilled with gases before each signal. Gases were allowed to stand for 5 min before each signal taken in order to ensure complete mixing. Typically, 2–8 laser shots per transient signal at a 1-Hz repetition rate were required. No significant depletion of reactants and only minor buildup of reaction products were observed under these conditions.

Bromine isocyanate was synthesized by the reaction of gaseous Br₂ with AgNCO at 420 K.²³ The sample was stored in a Pyrex bulb at 77 K. BrNCO was introduced into the reaction cell by briefly warming the storage bulb until a sufficient vapor pressure of sample had entered the reaction cell. ICN (Fluka) was purified by vacuum sublimation to remove dissolved air. SF₆ and CF₄ (Matheson) were purified by repeated freeze–pump–thaw cycles at 77 K. CO₂ and NO₂ (Matheson) were similarly purified at 150 and 200 K, respectively. Diode laser absorption at $\sim 1903 \text{ cm}^{-1}$ was used to analyze the NO₂ sample for NO impurity; typical impurity levels were 1%.

* To whom correspondence should be addressed.

• Abstract published in *Advance ACS Abstracts*, December 1, 1993.

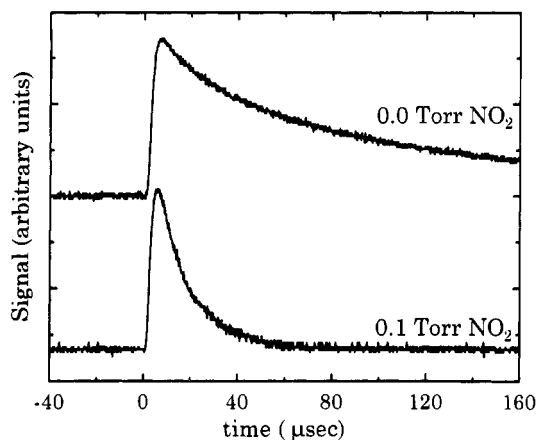
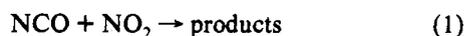
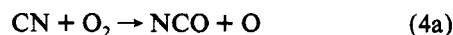
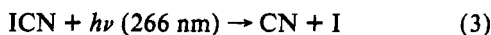


Figure 1. Transient infrared absorption signals for the NCO $P_{3/2}$ (13.5) line at 1909.59 cm^{-1} . Reaction conditions: $P_{\text{ICN}} = 0.2\text{ Torr}$, $P_{\text{O}_2} = 3.0\text{ Torr}$, $P_{\text{SF}_6} = 1.0\text{ Torr}$, and YAG pulse energy = 7.0 mJ . Upper trace: $P_{\text{NO}_2} = 0.0\text{ Torr}$. Lower trace: $P_{\text{NO}_2} = 0.1\text{ Torr}$.

Results

Total Rate Constant. The time-resolved concentration of NCO radicals was directly probed in order to measure the total rate constant for the reaction of NCO with NO_2 over the temperature range 298–500 K. For most of these experiments, ICN precursor molecules were used rather than BrNCO. This was necessary because thermal instability of BrNCO makes use of this species at elevated temperature difficult. Both precursors were found to give identical results at room temperature. When using ICN precursor, NCO radicals were produced by the rapid reaction of photolytically created CN radicals with molecular oxygen:



NCO was probed using the $P_{3/2}(13.5)$ line of the (000) \rightarrow (001) transition at roughly 1909.59 cm^{-1} . Typical reaction conditions were 0.2–0.3 Torr of ICN, 4.0 Torr of O_2 , 0–0.3 Torr of NO_2 , 2.0 Torr of SF_6 , and 3–8 mJ/pulse photolysis laser energy, producing NCO number densities of $\sim(1\text{--}5) \times 10^{13}$ molecules cm^{-3} . The large O_2 pressures were required because the $\text{CN} + \text{NO}_2$ reaction^{17,24} competes with the $\text{CN} + \text{O}_2$ reaction. Note that NCO does not react with O_2 .^{8,9} The reaction is pseudo-first-order with $[\text{NCO}] \ll [\text{NO}_2]$ under our conditions, so the time-dependent NCO concentration has the form

$$[\text{NCO}(t)] = [\text{NCO}]_0 \exp(-k't) = [\text{NCO}]_0 \exp(-k[\text{NO}_2]t) \quad (6)$$

This equation is valid only after reaction 4a is essentially complete. Figure 1 shows a typical transient signal of NCO radicals. The abrupt rise in the absorption signal is attributed to rapid formation of NCO by reaction 4a. Using $k_4 \approx 2 \times 10^{-11}$ molecule $\text{cm}^{-3}\text{ s}^{-1}$, at an O_2 pressure of 4.0 Torr, we predict a rise time of $\sim 0.4\ \mu\text{s}$. NCO products from reaction 4a are produced vibrationally hot,^{25,26} but the high pressure of SF_6 buffer gas used is expected to quickly relax any nascent vibrational or spin-orbit excitation to a Boltzmann distribution. The observed rise rate is thus a convolution of the rate of reaction 4 as well as vibrational relaxation rates and the $\sim 0.8\ \mu\text{s}$ detector time response.

The decay of the NCO absorption signal is attributed to the disappearance due to the reaction of NCO with NO_2 . The decay also includes secondary reactions (primarily reaction of NCO with precursor molecules, but also possibly including radical-radical reactions) and diffusion of NCO radicals out of the probed

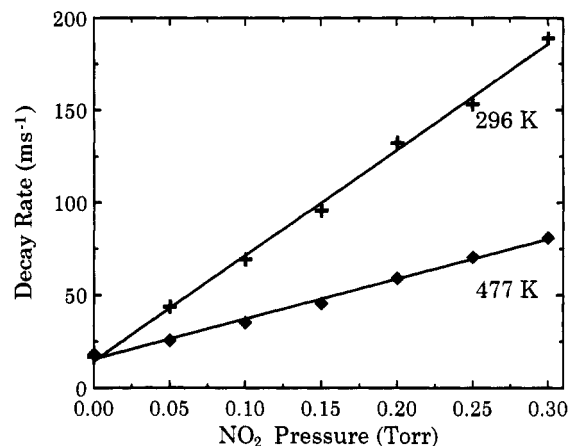


Figure 2. Pseudo-first-order decay rate of NCO radicals as a function of NO_2 pressure. Reaction conditions are the same as in Figure 1.

beam volume. At the total gas pressures used in this study, diffusion occurs on a time scale of $\sim 1\text{ ms}$, much slower than the observed decays. We therefore neglect diffusion in the analysis. The transient signals were fit to single-exponential decays to determine k' . Figure 2 shows the decay rate k' vs $[\text{NO}_2]$. As per standard kinetics, the slope of these plots gives the bimolecular rate constant of interest. At 296 K the rate constant was measured to be $(1.77 \pm 0.1) \times 10^{-11}$ $\text{cm}^3\text{ molecule}^{-1}\text{ s}^{-1}$; the uncertainty represents two standard deviations. The results were independent over factor of 2 changes in $[\text{ICN}]$ and photolysis laser pulse energy.

The temperature dependence of the total rate constant was measured in the range 296–500 K. As shown in the Figure 3, the rate of NCO with NO_2 decreased with increasing temperature. The data were found to fit the following Arrhenius expression over the measured temperature range:

$$k_1(T) = 10^{-11.38 \pm 0.06} \exp[(441 \pm 53)/T] \quad (7)$$

where the uncertainties represent one standard deviation.

Branching Ratio. Product branching ratios for the title reaction were measured by probing CO, CO_2 , NO, and N_2O reaction products by infrared adsorption spectroscopy. The following spectral lines were used:

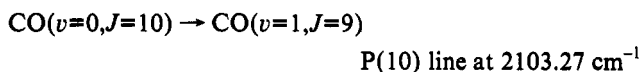
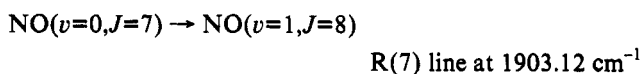
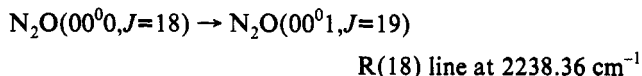
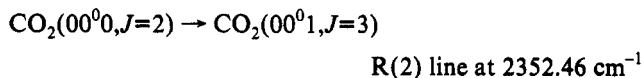


Figure 4 shows typical absorption signals of CO_2 , N_2O , CO, and NO obtained after photolysis of a ICN/ NO_2 / SF_6 gas mixture. The rise in the signal is due to the formation of the product, and the decay is due to the diffusion out of the probe beam volume.

To obtain molecular yields from a transient signal for a single ro-vibrational state, we must ensure that all product species are in a Boltzmann distribution. Two Torr of SF_6 buffer gas was therefore used to relax the nascent internal product state distribution. As documented in an earlier publication,¹⁹ SF_6 is efficient at relaxing vibrational excitation of CO_2 and N_2O ^{27,28} but inefficient at relaxing CO.^{29,30} CF_4 , however, has been shown to relax CO reasonably quickly.^{29,30} Our CO transient signals were found to be identical in magnitude and shape when CF_4 was

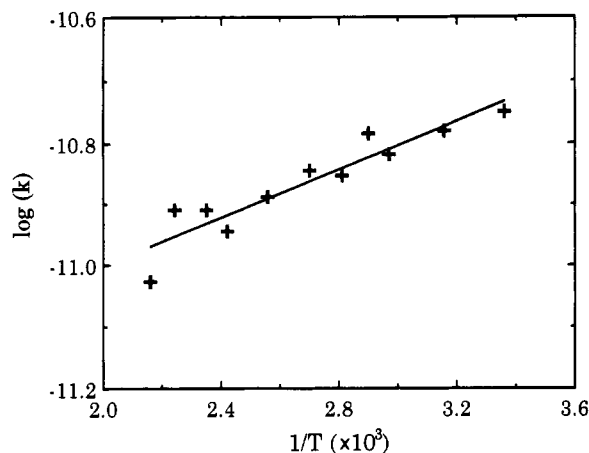


Figure 3. Arrhenius plot of the NCO + NO₂ reaction.

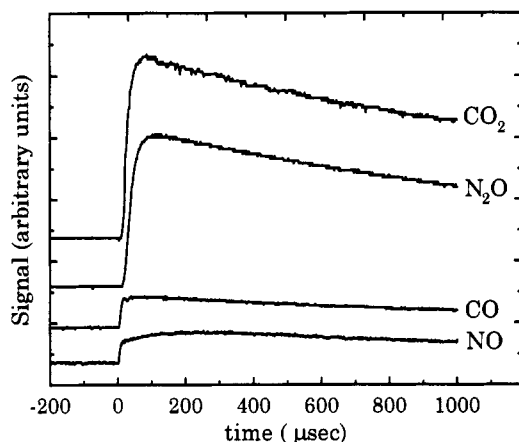


Figure 4. Transient infrared absorption signals for reaction products. $P_{\text{ICN}} = 0.1$ Torr, $P_{\text{NO}_2} = 0.3$ Torr, $P_{\text{SF}_6} = 2.0$ Torr, and YAG pulse energy = 7.0 mJ.

substituted for SF₆. This indicates that the nascent CO products either are formed vibrationally cold or quickly relax via collisions with other gases in the mixture. We have also directly measured the population of CO in the $v = 1$ state (using the $v = 1$, P(10) line at 2077.14 cm⁻¹) using Ar rather than SF₆ buffer gas, which is expected to efficiently relax rotational but not vibrational motion. It was found that the CO yield in the $v = 1$ state was less than 2% of the total CO yield. The NO signal in Figure 4 displays both fast ($\tau \sim 10$ μs) and slow ($\tau \sim 80$ μs) rise components. When the $v = 1$, R(17.5) line of NO at 1902.989 cm⁻¹ was probed (not shown), the transient signal showed a decay time similar to the slower rise time in the $v = 0$ signals. This indicates that the slow rise component is due to the relaxation from vibrationally excited NO molecules. We therefore conclude that the quantum state distributions of all probed product molecules were fully thermalized in the first 100–150 μs.

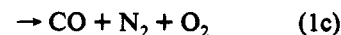
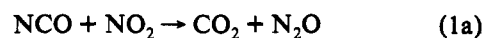
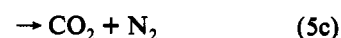
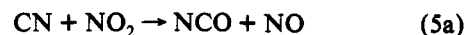
The transient decay portion of each signal was fit to a double-exponential decay in order to approximate the effect of diffusion of product molecules out of the probed beam volume. Although cylindrical diffusion does not strictly follow an exponential decay, this was found to be a sufficiently good approximation for our purposes. The resulting decay term was extrapolated to $t = 0$ in order to obtain the signal amplitude which would be expected in the absence of diffusion; this was typically only a $\sim 10\%$ correction. From this signal amplitude, the number density N_{vJ} of product molecules in the probed rotation–vibration state was calculated as previously described¹⁹ using standard formulas and tabulated line strengths.^{20,21} Note that pressure broadening is insignificant at the total pressures (2.2–2.5 Torr) used in the product yield experiments. The total number density of product molecules is

then

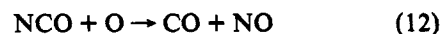
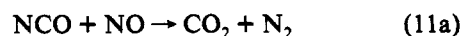
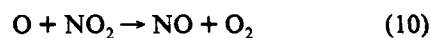
$$N = N_{vJ}/f_v f_J \quad (8)$$

where f_v and f_J are the fraction of total molecules in the probed vibrational and rotational state, respectively. These are calculated by assuming a room temperature Boltzmann distribution of product states. As discussed in earlier publications,^{18,19} transient heating effects have an insignificant effect on the product yield determination, because we avoid the use of high rotational states which would be sensitive to small temperature changes.

Two different precursors, ICN and BrNCO, were used to obtain the product branching ratios. In the first method, transient number densities of CO, CO₂, N₂O, and NO were measured after photolysis of an ICN/NO₂/SF₆ mixture. The primary reactions under these conditions are



Typical conditions are $P_{\text{ICN}} = 0.05$ – 0.15 Torr, $P_{\text{NO}_2} = 0.2$ – 0.4 Torr, and $P_{\text{SF}_6} = 2.0$ Torr. Note that, unlike the total rate constant experiments, O₂ is not present in the reaction mixture. Instead, NCO is formed by reaction 5a. As shown in a previous publication,¹⁷ NCO + NO is the primary product channel in reaction 5, but channels 5b and 5c are also present with branching ratios of 0.076 and 0.056, respectively, and must be included in the analysis. Several other possible secondary reactions include



Reactions 9 and 10 produce a small amount of background NO signal which is observed by photolyzing an NO₂/SF₆ mixture. This signal was about 25% of the NO signal measured when ICN was included in the reaction mixture. The effect of these reactions was taken into account by subtraction of the background signal. The other reactions are expected to be negligible compared to reactions 1 and 5 because they involve species in low concentrations. Simple kinetic modeling calculations have confirmed that we are justified in ignoring reactions 11–14.

Even when only considering reactions 1 and 5, several simplifications are necessary in order to obtain branching ratios from the product yield data. First, we assume that every NCO molecule produced in reaction 5a reacts with NO₂ via reaction 1. This is clearly a valid assumption only in the limit of high NO₂

pressure. The kinetic plots of Figure 2 show that, in the absence of NO₂, NCO has a first-order decay constant of roughly 15 ms⁻¹ under our conditions, due to NCO decay routes other than reaction 1. At an NO₂ pressure of 0.2 Torr, we see that this decay rate increases to 130 ms⁻¹. Thus, this approximation is correct to within 10% if the NO₂ pressure used is ~0.2 Torr or greater. The pressures used in the product yield experiments represent a trade-off between the necessity to ensure this condition with the requirement to minimize background from NO₂ photodissociation, reactions 9 and 10.

The second approximation in the analysis is to neglect any product yield from channel 1c. This assumption will be experimentally justified later. The analysis then closely follows the treatment used in our earlier study of the CN + NO₂ reaction.¹⁷ In the experiment, we directly measure total number densities [NO]_{tot}, [CO]_{tot}, [N₂O]_{tot}, and [CO₂]_{tot}. We can then write the following mass balance equations:

$$[\text{CO}_2]_{\text{tot}} = [\text{CO}_2]_{5c} + [\text{CO}_2]_{1a} \quad (15)$$

$$[\text{N}_2\text{O}]_{\text{tot}} = [\text{N}_2\text{O}]_{5b} + [\text{N}_2\text{O}]_{1a} \quad (16)$$

$$[\text{NO}]_{\text{tot}} = [\text{NO}]_{5a} + [\text{NO}]_{1b} \quad (17)$$

$$[\text{CO}]_{\text{tot}} = [\text{CO}]_{5b} + [\text{CO}]_{1b} \quad (18)$$

$$[\text{NCO}]_{5a} = [\text{CO}_2]_{1a} + [\text{CO}]_{1b} \quad (19)$$

where [CO₂]_{tot} is the total number density of CO₂ products, [CO₂]_{5c} is the number density of CO₂ originating from reactions 5c, etc. Using the fact that [CO₂]_{1a} = [N₂O]_{1a}, [NO]_{1b} = 2[CO]_{1b}, etc., we can solve these equations to obtain the yield of products in reaction 1:

$$[\text{N}_2\text{O}]_{1a} = \frac{[\text{NO}]_{\text{tot}} + 3[\text{N}_2\text{O}]_{\text{tot}} - 3[\text{CO}]_{\text{tot}}}{4} \quad (20)$$

$$[\text{CO}]_{1b} = \frac{[\text{NO}]_{\text{tot}} - [\text{N}_2\text{O}]_{\text{tot}} + [\text{CO}]_{\text{tot}}}{4} \quad (21)$$

The product branching ratios are then defined as

$$\phi_{1a} = \frac{[\text{N}_2\text{O}]_{1a}}{[\text{N}_2\text{O}]_{1a} + [\text{CO}]_{1b}} \quad (22)$$

$$\phi_{1b} = \frac{[\text{CO}]_{1b}}{[\text{N}_2\text{O}]_{1a} + [\text{CO}]_{1b}} \quad (23)$$

In order to test some of the assumptions made above, we performed additional experiments using BrNCO precursor molecules, which directly photolyze to produce vibrationally cold NCO.³¹ For these experiments, the reaction mixture consists of BrNCO, NO₂, and SF₆ buffer gas. Unfortunately, our BrNCO samples contained a significant CO₂ impurity which proved difficult to remove. We could therefore probe only N₂O, NO, and CO products. The only secondary reactions considered were reactions 9 and 10. These were treated by background subtraction, as before. After this correction, the NO yield was observed to be 1.7 ± 0.4 times that of the CO yield. If channel 1b is active but channel 1c is negligible, one expects [NO] = 2[CO] under these conditions. Our result is thus consistent with neglecting channel 1c, but we cannot exclude the possibility that channel 1c is a minor contribution. An estimated upper limit for φ_{1c} is 0.04. The resulting branching ratios for channels 1a and 1b, obtained from the ratio of [N₂O] and [CO] yields, are shown in Table 1. As shown, the branching ratios obtained with BrNCO and ICN precursor are in remarkable agreement. Our results were also independent of the exact reaction conditions used, such as NO₂ pressure (varied from 0.2 to 0.4 Torr) and photolysis pulse laser energy (varied from 3 to 8 mJ/pulse). The N₂O + CO₂ channel

TABLE 1: Branching Ratios of the NCO + NO₂ Reaction

NCO precursor	branching ratio ^a		rate constant ^b	
	Φ _{1a}	Φ _{1b}	k _{1a}	k _{1b}
ICN	0.912 ± 0.05	0.088 ± 0.04	1.64 × 10 ⁻¹¹	0.13 × 10 ⁻¹¹
BrNCO	0.922 ± 0.01	0.078 ± 0.05	1.63 × 10 ⁻¹¹	0.14 × 10 ⁻¹¹

^a Data at 296 K. Uncertainties represent 1.5σ. Product branching ratios are defined as Φ_{1a} = k_{1a}/(k_{1a} + k_{1b}), etc. ^b In cm³ molecule⁻¹ s⁻¹. Assuming that k_{1a} + k_{1b} = 1.77 × 10⁻¹¹ cm³ molecule⁻¹ s⁻¹.

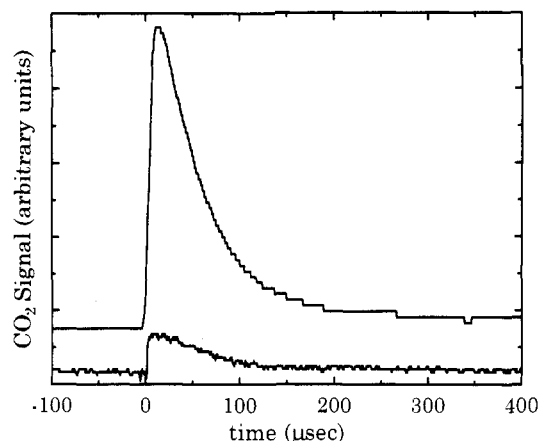
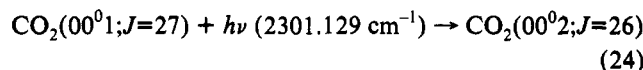


Figure 5. Transient infrared absorption signal for CO₂ in the (00⁰₁) P(27) line at 2301.129 cm⁻¹ under harvesting conditions (see text). Upper trace: P_{BrNCO} = 0.06 Torr, P_{NO₂} = 0.2 Torr, P_{CO₂} = 2.0 Torr, and YAG pulse energy = 7.0 mJ. Lower trace: same conditions except P_{NO₂} = 0.0 Torr.

clearly dominates this reaction, with a minor contribution from the CO + 2NO.

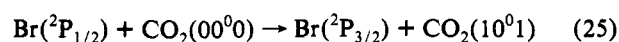
Energy Disposal. Vibrational energy disposal into the CO₂ products was studied using a “quantum harvesting” technique previously described.^{19,32} For these experiments, BrNCO precursor was used. The P(27) line of the CO₂(00⁰₁) hot band was probed:



Typical reaction conditions of 0.05–0.07 Torr of BrNCO, 0.1–0.5 Torr of NO₂, and 2.0 Torr of CO₂ were used. Product CO₂ molecules produced in reaction 1a collide primarily with CO₂ buffer gas. Under these conditions, intramode vibrational relaxation in CO₂ takes place quickly, but intermode (V–V) and (V–R,T) energy transfer takes place much more slowly.³² Probing the metastable (00⁰₁) state therefore provides an estimate of the amount of reaction exoergicity deposited into the ν₃ antisymmetric stretching mode.

A typical transient signal of CO₂ products in the (00⁰₁) state taken under harvesting condition is shown in Figure 5. As mentioned earlier, the rise of the transient signal represents the accumulation of CO₂ in the (00⁰₁) state by intramode (V–V) processes. The decay of the transient signal represents the relaxation of CO₂ out of the (00⁰₁) vibrational state. The decay rate was observed to increase with increasing BrNCO pressure, suggesting that some of this relaxation is due to BrNCO.

The lower trace in Figure 5 shows the CO₂ absorption signal in the (00⁰₁) state without NO₂ gas. This signal is presumably due to nonreactive excitation mechanisms such as³³



The signal due to nascent ν₃ excitation of CO₂ reaction products was therefore estimated by the subtraction from this background signal created in the absence of NO₂ gas. Calculation of the CO₂(00⁰₁) number densities from the transient signal was accomplished in a similar manner to the branching ratio data.

TABLE 2: Energy Disposal into the ν_3 Mode of CO₂

	experimental	prior distribution
no. of ν_3 quanta/CO ₂	1.06 ± 0.14	1.56
% available energy	5.9 ± 2.0	8.7

The harvesting data indicate that the energy disposal of reaction 1a into the ν_3 mode is 1.06 ± 0.14 quanta/CO₂ molecule (see Table 2). Assuming $\Delta H = -500.57$ kJ/mol and no potential energy barrier, and allowing for possible systematic errors, this is equivalent to roughly $5.9 \pm 2\%$ of the available energy.

Discussion

The observed branching ratios may be rationalized on the basis of the likely structure of the initially formed collision complex. Prior experimental studies on the NCO + NO reaction^{18,19,34} as well as recent BAC-MP4 calculations³⁵ indicated that a bent ONNCO complex could undergo facile rearrangement to a cyclic structure in which the carbon atom is bound to both oxygen atoms. Concerted dissociation via a four-center transition state then leads to CO₂ + N₂ products in high yield. A similar mechanism involving an O₂NNCO complex is probably active in the NCO + NO₂ reaction as well. The additional oxygen atom in NO₂ remains bound to nitrogen, leading to CO₂ + N₂O products. The minor CO + 2NO channel most likely involves an ONONCO complex in which both the N–C and an N–O bond break (not necessarily simultaneously). Formation of CO + N₂ + O₂ would require highly unlikely rearrangements involving a three-center transition state; it is therefore not surprising that this channel is not observed.

It is worthwhile to consider other possible product channels other than (1a), (1b), or (1c). Attack on the oxygen end of NCO would be expected to lead to CN + NO₃ or possibly CN + NO + O₂ products. As these reactions are endothermic by 342.0 and 361.2 kJ/mol, respectively, they are not accessible at moderate temperatures. It is thermodynamically possible, however, for CO₂ or N₂O formed in channel 1a to dissociate, forming CO + O + N₂O or CO₂ + N₂ + O. In earlier studies on the related NCO + NO reaction, such a process was initially believed to play a minor role¹⁸ but was later found to be insignificant.^{19,34} Our data here cannot completely exclude these channels, because both CO₂ and N₂O originate from more than one reaction when the ICN precursor is used. When BrNCO precursor was used, CO₂ impurity levels prevent a direct comparison of CO₂ and N₂O product yields. We do observe approximately equal [CO₂] and [N₂O] yields when using ICN, suggesting that CO₂ + N₂ + O or CO + O + N₂O represent at most minor contributions to the overall reaction.

A potential source of error in the measurement of total rate constants for the NCO + NO₂ reaction is NCO loss by secondary reactions. NCO does not react with O₂ but does react quite quickly with nitric oxide.^{5–8,18,19} There are several sources of NO in this experiment: it is a product of reactions 4b, 1b, and 5a, it is produced the photodissociation of NO₂ (reaction 9), and it is initially present as a ~1% impurity in the NO₂ samples. The amount of NO present will therefore depend on the NO₂ pressure used, so the NCO + NO reaction could in principle affect the slopes in Figure 2. We have therefore performed kinetic modeling calculations using standard software³⁶ to investigate this possibility. We have included reactions 1, 3–5, and 7–11 in the model and assumed typical conditions of 5 mJ YAG pulse energy, 0.2 Torr of ICN, and 0.3 Torr of NO₂. All sources of NO described above were included in the calculation. We find that inclusion of the NCO + NO reaction increases the NCO decay rate by only 4%. As this is less than the quoted uncertainty limits on k_1 , we conclude that the presence of NO in our experiment does not significantly affect the rate constant measurements.

Except for reaction with NO,^{5–8} comparatively few previous workers have reported kinetic data for NCO reactions.^{9–11,37} A

very recent flow reactor study has reported $k_1 = (7.52 \pm 0.49) \times 10^{-12}$ cm³ molecule⁻¹ s⁻¹ at room temperature.³⁷ This is roughly a factor of 2 smaller than our result of $(1.77 \pm 0.1) \times 10^{-11}$ cm³ molecule⁻¹ s⁻¹ reported here. At present, we have no explanation for this discrepancy, although we note that neither study has seriously investigated the possibility of a pressure-dependent rate constant. In any case, the rate constant is several times smaller than that for the NCO + NO reaction, which has been measured by several workers^{5–8} to be $(3.2–3.4) \times 10^{-11}$ cm³ molecule⁻¹ s⁻¹. A possible rationalization for this fact is that an O₂NNCO complex must rearrange to a cyclic structure in order to form stable products. This is in contrast to an ONNCO complex, in which both concerted dissociation of a cyclic intermediate and simple fission of the N–C bond are viable reaction mechanisms. A negative activation energy is observed for both the NCO + NO and NCO + NO₂ reactions, as is expected for reactions involving long-range attractive forces in the entrance channel.

It is useful to compare our harvesting data to simple statistical models of energy disposal. Reaction 1a corresponds to the case of two linear triatomic reaction products, for which a statistical prior model³⁸ predicts $\langle f_{\nu_3} \rangle = 2/23 = 8.70\%$. This is quite close to our experimental value for the energy deposition into the ν_3 mode of CO₂. This observation is consistent with initial formation of an O₂NNCO complex. Energy is randomized as the complex rearranges to a four-center structure and dissociates.

Conclusion

The kinetics and product channels of the NCO + NO₂ reaction have been studied. The reaction is fast but with a negative activation energy and leads primarily to N₂O + CO₂ products, with a minor contribution from the CO + 2NO product channel. The kinetic and energy disposal data are consistent with O₂NNCO complex formation in a deep potential well, followed by a concerted dissociation mechanism leading to the primary products.

Acknowledgment. The authors thank M. C. Lin (Emory) and Don Setser (Kansas State) for making results available prior to publication. This work was partially supported by the Division of Chemical Sciences, Office of Basic Energy Sciences, of the Department of Energy (Contract No. DE-FG06-93ER14390). Acknowledgment is also made to the donors of the Petroleum Research Fund, administered by the American Chemical Society, for partial support of this research.

References and Notes

- (1) Miller, J. A.; Bowman, C. T. *Prog. Energy Combust. Sci.* **1989**, *15*, 287.
- (2) Miller, J. A.; Bowman, C. T. *Int. J. Chem. Kinet.* **1991**, *23*, 289.
- (3) Perry, R. A.; Siebers, D. L. *Nature* **1986**, *324*, 657.
- (4) Siebers, D. L.; Caton, J. A. *Combust. Flame* **1990**, *79*, 31.
- (5) Perry, R. A. *J. Chem. Phys.* **1985**, *82*, 5485.
- (6) Cookson, J. L.; Hancock, G.; McKendrick, K. G. *Ber. Bunsen-Ges. Phys. Chem.* **1985**, *89*, 335.
- (7) Hancock, G.; McKendrick, K. G. *Chem. Phys. Lett.* **1986**, *127*, 125.
- (8) Atakan, B.; Wolfrum, J. *Chem. Phys. Lett.* **1991**, *178*, 157.
- (9) Perry, R. A. *Symp. (Int.) Combust.* **1986**, *25*, 913.
- (10) Louge, M. Y.; Hanson, R. K. *Combust. Flame* **1984**, *58*, 291.
- (11) Louge, M. Y.; Hanson, R. K. *Symp. (Int.) Combust.* **1984**, *20*, 665.
- (12) East, A. L. L.; Allen, W. D. *J. Chem. Phys.* **1993**, *99*, 4638.
- (13) Chase, M. W., Jr.; et al. *JANAF Thermochemical Tables*, 3rd ed.; *J. Phys. Chem. Ref. Data* **1985**, *14* (Suppl. 1).
- (14) de Juan, J.; Smith, I. W. M.; Veyret, B. *J. Phys. Chem.* **1987**, *91*, 69.
- (15) Durant, J. L., Jr.; Tully, F. P. *Chem. Phys. Lett.* **1989**, *154*, 568.
- (16) Atakan, B.; Jacobs, A.; Wahl, M.; Weller, R.; Wolfrum, J. *Chem. Phys. Lett.* **1989**, *154*, 449.
- (17) Park, J.; Hershberger, J. F. *J. Chem. Phys.* **1993**, *99*, 3488.
- (18) Cooper, W. F.; Hershberger, J. F. *J. Phys. Chem.* **1992**, *96*, 771.
- (19) Cooper, W. F.; Park, J.; Hershberger, J. F. *J. Phys. Chem.* **1993**, *97*, 3283.
- (20) Rothman, L. S.; et al. *Appl. Opt.* **1987**, *26*, 4058.
- (21) Rothman, L. S.; et al. *Appl. Opt.* **1983**, *22*, 2247.

- (22) Brueggemann, R.; Petri, M.; Fischer, H.; Mauer, D.; Reinert, D.; Urban, W. *Appl. Phys. B* **1989**, *48*, 105.
- (23) Gottardi, W. *Angew. Chem., Int. Ed. Engl.* **1971**, *10*, 416.
- (24) Wang, N. S.; Yang, D. L.; Lin, M. C. *Chem. Phys. Lett.* **1989**, *163*, 480.
- (25) Sauder, D. G.; Patel-Misra, D.; Dagdigian, P. J. *J. Chem. Phys.* **1991**, *95*, 1696.
- (26) Phillips, L. F.; Smith, I. W. M.; Tuckett, R. P.; Whitham, C. J. *Chem. Phys. Lett.* **1991**, *183*, 254.
- (27) Fakhr, A.; Bates, R. D., Jr. *Chem. Phys. Lett.* **1980**, *71*, 381.
- (28) Stephenson, J. C.; Moore, C. B. *J. Chem. Phys.* **1970**, *52*, 2333.
- (29) Richman, D. C.; Millikan, R. C. *J. Chem. Phys.* **1975**, *63*, 2242.
- (30) Green, W. H.; Hancock, J. K. *J. Chem. Phys.* **1973**, *59*, 4326.
- (31) Liu, X.; Gilbert, J. V.; Coombe, R. D. *J. Chem. Phys.* **1989**, *90*, 171.
- (32) Mandich, M. L.; Flynn, G. W. *J. Chem. Phys.* **1980**, *73*, 1265.
- (33) Haugen, H. K.; Weitz, E.; Leone, S. R. *J. Chem. Phys.* **1985**, *83*, 3402.
- (34) Becker, K. H.; Kurtenbach, R.; Wiesen, P. *Chem. Phys. Lett.* **1992**, *198*, 424.
- (35) Lin, M. C.; He, Y.; Melius, C. F. *J. Phys. Chem.* **1993**, *97*, 9124.
- (36) Braun, W.; Herron, J. T.; Kahaner, K. *Int. J. Chem. Kinet.* **1988**, *20*, 51.
- (37) Wategaonkar, S.; Setser, D. W. *J. Phys. Chem.* **1993**, *97*, 10028.
- (38) Muckermann, J. T. *J. Phys. Chem.* **1989**, *93*, 179.